Making corrections to your proof

Please follow these instructions to mark changes or add notes to your proof. Ensure that you have downloaded the most recent version of Acrobat Reader from **https://get.adobe.com** so you have access to the widest range of annotation tools.

The tools you need to use are contained in **Annotations** in the **Comment** toolbar. You can also right-click on the text for several options. The most useful tools have been highlighted here. If you cannot make the desired change with the tools, please insert a sticky note describing the correction.

Please ensure all changes are visible via the 'Comments List' in the annotated PDF so that your corrections are not missed.

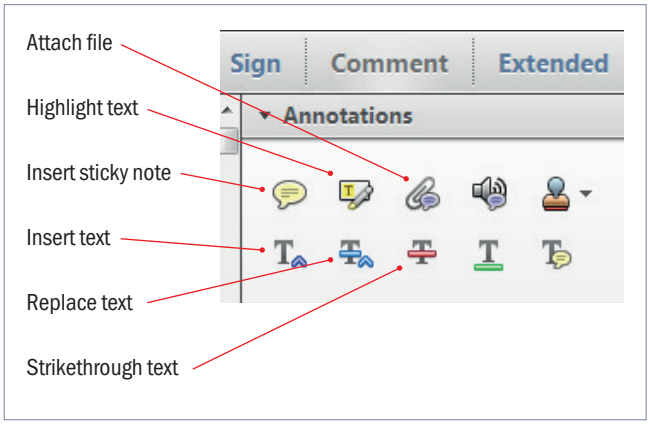

Do not attempt to directly edit the PDF file as changes will not be visible.

Replacing text

To replace text, highlight what you want to change then press the replace text icon, or right-click and press 'Add Note to Replace Text', then insert your text in the pop up box. Highlight the text and right click to style in bold, italic, superscript or subscript.

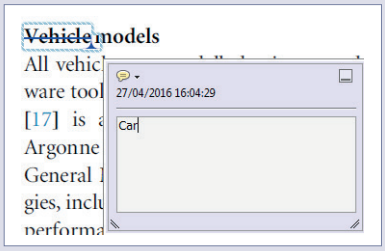

Inserting text

Place your cursor where you want to insert text, then press the insert text icon, or right-click and press 'Insert Text at Cursor', then insert your text in the pop up box. Highlight the text and right click to style in bold, italic, superscript or subscript.

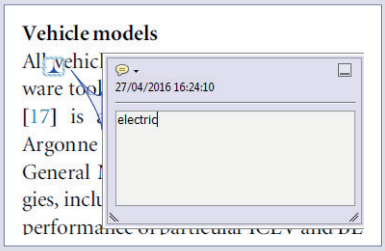

Deleting text

To delete text, highlight what you want to remove then press the strikethrough icon, or right-click and press 'Strikethrough Text'.

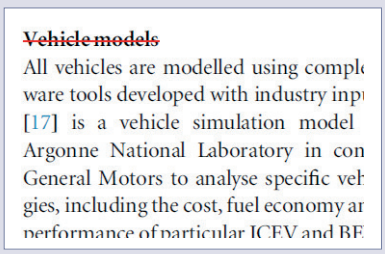

Highlighting text

To highlight text, with the cursor highlight the selected text then press the highlight text icon, or right-click and press 'Highlight text'. If you double click on this highlighted text you can add a comment.

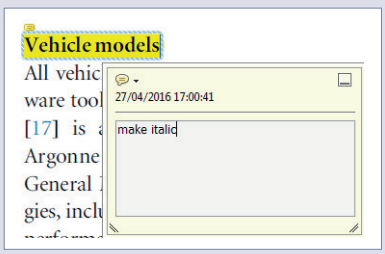

QUERIES

Page 1
AQ1
Please check that the names of all authors as displayed in the proof are correct, and that all authors are linked correctly to the appropriate affiliations. Please also confirm that the correct corresponding author has been indicated.
AQ2
Reference [23] is a duplicate of [8] and hence the repeated version has been deleted. Please check.
Page 2
AQ3
We have changed the units from "[A°, mv/s]" to "[Å, mV s^{-1}]". Please check and confirm.
Page 10
AQ4
If an explicit acknowledgment of funding is required, please ensure that it is indicated in your article. If you already have an Acknowledgments section, please check that the information there is complete and correct.
Page 11
AQ5
Please check the details for any journal references that do not have a link as they may contain some incorrect information. If any journal references do not have a link, please update with correct details and supply a Crossref DOI if available.

Materials Research Express

PAPER

Effect of heat treatment on corrosion behavior of duplex stainless steel in orthodontic applications

RECEIVED
5 September 2017

REVISED
9 November 2017

ACCEPTED FOR PUBLICATION
21 November 2017

PUBLISHED AQ1

Ali Sabea Hammood[1], Ahmed Faraj Noor[1] and Mohammed Talib Alkhafagy[2]

[1] Faculty of Engineering, Material Engineering Department, University of Kufa, Iraq
[2] Faculty of Dentistry, University of Kufa, Iraq

E-mail: alis.altameemi@uokufa.edu.iq, ahmedf.aljabery@student.uokufa.edu.iq and mohamedta@uokofa.edu.iq

Keywords: duplex stainless steel, heat treatment, artificial saliva, cyclic potentiodynamic, orthodontic wire

Abstract

Heat treatment is necessary for duplex stainless steel (DSS) to remove or dissolve intermetallic phases, to remove segregation and to relieve any residual thermal stress in DSS, which may be formed during production processes. In the present study, the corrosion resistance of a DSS in artificial saliva was studied by potentiodynamic measurements. The microstructure was investigated by scanning electron microscopy (SEM) ,x-ray diffraction (XRD) and Vickers hardness (HV). The properties were tested in as–received and in thermally treated conditions (800–900 °C, 2–8 min). The research aims to evaluate the capability of DSS for orthodontic applications, in order to substitute the austenitic grades. The results indicate that the corrosion resistance is mainly affected by the ferrite/austenite ratio. The best result was obtained with a treatment at 900 °C for 2 min.

1. Introduction

Duplex stainless steels (DSS), which consist of two-phase austenite–ferrite microstructures, are essential for many applications such as gas refineries, petroleum, and marine media, due to their excellent mechanical properties and corrosion resistance [1–5]. Chromium (Cr) and molybdenum (Mo) are ferrite stabilizer elements, while nitrogen (N) and nickel (Ni) are primarily enriched in austenite [6]. The DSS exhibits complicated phase transformations and precipitation behavior since it contains high alloying elements [7]. Generally, the optimum properties can be obtained with around an equal volume fraction of austenite and ferrite without secondary phases, such as a sigma phase [7]. The DSSs have high mechanical strength and good corrosion resistance properties, with relatively low cost [8]. AQ2

DSS was found be employed in corrosive media, due to its microstructure which has equal amounts of austenite and ferrite phase. This phase combination can lead to good properties such as toughness, hardness and corrosion resistance [9].

Furthermore, 2205 DSSs have a nickel content lower than traditional austenitic stainless steels, with higher strength and acceptable plasticity. The low nickel content may suggest its use duplex as a biomaterial, in order to eliminate or to reduce the risk of Ni allergic reaction [10]. Many authors have studied the corrosion behavior of DSS under different conditions [11–13].

In respect of the biomedical application, a study [14] confirms that the corrosion resistance characteristics of 2205 DSS are better than those of AISI 316L stainless steel, especially under potentiodynamic conditions.

Nickel allergy constitutes a serious health problem in modern societies. Hypersensitivity to this metal is found in 13% of adults and 8% of children. Risk factors for nickel allergy are: females with early exposure to nickel, e.g. piercing. Various mechanisms to induce nickel allergy are possible, which is also reflected in the different clinical pictures. Though an allergic response to nickel in the oral mucosa from nickel containing orthodontic appliances is more infrequent than from nickel contact on the epidermis, it can occur, particularly in females [28]. The present study aims to explore the effect of heat treatment on the electrochemical behavior of DSS 2205 in artificial saliva.

Table 1. The chemical composition analysis of 2205 DSS alloys as received, wt. %.

Alloy	ASTM	Cr	Ni	Mo	C	N	Fe
2205	S32205	22.4	5.7	3.1	0.02	0.17	Balance

2. Experimental procedure

2.1. Material and heat treatment

In the present work, super DSS plates SAF 2205 are employed. The chemical composition is listed in table 1. Solution treatment was first performed at 1150 °C for 15 min (for all samples), in the tube furnace, followed by water quenching in accordance with ASTM A182.

This solution treatment is necessary to eliminate secondary phases, to balance the phase fractions and to release any residual stress during production processes. The solubilized samples were heat treated at 800 °C for (2, 4, 8 min), at 850 °C for 2 min and at 900 °C for 2 min, then were water quenched.

2.2. Light microscopy (LM)

The preparation of specimens for microstructural examination was performed according to ASTM standard (E3-01). The preparations' procedures include many steps such as mounting and the surfaces of the samples, including the edges, were wet ground using 120, 220, 320, 600, 1000, 1200, 2000 and 2500 grit silicon carbide papers. Next these samples were rinsed in distilled water, then polished with a diamond paste of 0.9, 0.3 μm to obtain a mirror-like surface for the final step. After polishing, the specimens were cleaned with ultrasonic devices by ethanol media for 10 min. The electrochemical etching was carried out with a solution containing 40 g of NaOH +100 ml of distilled water, at 2 V for 10 s (immersion time) with the platinum cathode electrode and the sample acting as an anode. Light microscopy (LM) can reveal the changes in ferrite and austenite phases and detect the presence of third phases.

2.3. Scanning electron microscopy (SEM)

SEM is used to identify surface morphology features as well as to better characterize the microstructural characteristics associated with the austenite, ferrite, and intermetallic phases. In addition, the chemical compositions of samples were performed by energy dispersive spectroscopy (EDS). In the present work, the test has been carried out in the materials laboratory in the Al-Razi Metallurgy Research Center by using SEM type (TM = 1000 Hitachi table top Japan).

2.4. Vickers micro-hardness test

A hardness test was carried out using a Vickers micro hardness tester Machine (TH715. Beijing Time High Technology Ltd), with an attached microscope, at 400X total magnification according to ASTM E 384-99.

2.5. X-ray diffraction (XRD)

X-ray diffraction was used for phases' identification (The SHIMADZU LabX XRD-6000, Japan x-ray), with a nickel filter and Cu Kα radiation ($\lambda = 1.5406$ Å). The scanning speed of the diffract-meter was adjusted to 6° min^{-1} with the range of the diffraction angle $2\theta°$ being (40°–100°). AQ3

2.6. Electrochemical corrosion tests

Two types of corrosion tests were performed in artificial saliva, the composition of which is presented in table 2 [27]. The first one is potentiodynamic polarization by using a three-electrode electrochemical cell, with a platinum counter electrode and a saturated calomel reference electrode (SCE) and the working electrode (DSS). The cell contains an electrolyte, which simulates the natural saliva. According to (ASTM G5-94 Reapproved 1999 updated 2002), polarization tests were performed of the potentiostat type (Winking M Lab 200). The second cyclic potentiodynamic polarization technique was used to determine the pitting behavior of the 2205 DSS.

The specimens were prepared into discs with a 1 cm^2 surface area and 2 mm height. All samples, prior to tests, were ground with SiC paper up to 3000 grit, then polished. After polishing, the specimens were cleaned with ethyl alcohol and dried with an air stream. Prior to testing, all specimens were immersed in the electrolytes and the cell was left to stabilize the open circuit potential (OCP). The potential scanning rate was 1 mV s^{-1} and the scanning rate was (−300 to 200) mV versus a saturated Calomel electrode.

2.7. Dissolution and release of Ni-ions test

This test was done by using an atomic absorption spectroscopy device. In order to evaluate the amount of Ni ions released from the 2205 DSS samples, before and after heat treatment into artificial saliva solution, the ions'

Table 2. The artificial saliva solution composition.

Compound	Composition (mg 100 ml^{-1})
NaCl	40.0
KCl	40.0
$Na_2HPO_4H_2O$	69.0
$Na_2S.9H_2O$	0.5
CaCl2·2H2O	79.5
$CO(NH_2)_2$	100.0

release test was used to determine the ions in the artificial saliva solution from the samples immersed for 4 weeks at 37 °C.

3. Results and discussion

3.1. Effect of solution treatment on microstructure and phases fraction

The micrograph of the 2205 DSS, as in figure 1(a), shows that the microstructure for the untreated specimen contains only ferrite and austenite and no secondary phases were observed. The ferrite appears darker than the austenite on the micrograph. Quantitative analysis of the microstructure, using a MIP4 student material program, gave an area fraction of 50.5% ferrite and 49.5% austenite.

After heat treatment, secondary phases can be formed and will subsequently influence the corrosion and mechanical properties of the material in service conditions. The type of secondary phases and its volume fraction depend on many factors such as ageing temperature, and ageing time. The heat treatment temperature and time effect of 2205 DSS can be seen in figure 1. When 2205 DSS is treated by a temperature less than the solution annealing temperature, the metastable thermodynamic balance was discomposure, resulting in the material trying for a more stable thermodynamic state through the precipitation of secondary phases. Sigma phase preferentially nucleated at the α/γ or α/α interfaces and grew through the adjacent ferrite, due to the ferrite phase being unstable at high temperatures. This is because the diffusion rates of alloying elements such as Cr and Mo are 100 times faster than the diffusion rates values in the austenite. Intermetallic did not appear when 2205 DSS was treated at 800 °C for 2, 4, 8 min, and at 850 °C for 2 min, as shown in figures 1(b)–(e). This result concurs with Calliari *et al* [15], who estimated that the sigma phase appears after about 10 min when 2205 DSS has aging at 850 °C.

The specimen treated at 900 °C for 2 min also contained ferrite and austenite only but secondary phases did not appear, as shown in figure 2(f).

3.2. Effect of heat treatment on microstructural morphology and distribution of phases

The effect of the heat treatment on the constituent phase's morphology of specimens was characterized by the SEM. In addition, figure 2 shows the morphology of 2205 DSS samples before and after being treated at different heat treatment conditions. The darker region represents the ferrite phase and the brighter region represents the austenite phase. Figure 2(a) illustrates that the as-received sample did not show any secondary precipitates where it contains ferrite and austenite only. In other words, this sample was not sensitized to precipitate. Figures 2(b)–(f) illustrate the SEM micrograph of the specimens treated at 800 °C for 2 min, 800 °C for 4 min 800 °C for 8 min, 850 °C for 2 min and 900 °C for 2 min respectively. It shows that the samples treated at these conditions were not sensitive to intermetallic precipitations where they had ferrite and austenite. Conversely, the heat treatment has an effect on the ferrite and austenite volume fraction and its grain size. The volume fraction of the ferrite phase increased with increasing the ageing temperature and the ageing time influenced directly the volumetric concentrations of the ferrite and austenite phases. The volume fraction of the austenite phase increased with time and this result is in good agreement with Badji *et al* [16]. The other effect of heat treatment that appeared with increasing the aging temperature was the increase of ferrite grain size.

3.3. Phases identification by XRD

Identification of prescience phases for 2205 DSS samples, before and after being heat treated, was carried out by x-ray diffraction technique. Figure 3 shows the diffraction patterns of 2205 DSS samples before being treated and samples treated at 800 °C for 2, 4 min. The three diffraction patterns show the peaks corresponding to the ferrite and austenite phases only; no evidence was observed for the sigma phase and this result is in agreement with Fargas [17]. The examination of the DSS samples evidenced the effect of the annealing temperature on the microstructure. Peaks corresponding to ferrite and austenite were clearly observed in the XRD pattern, whereas the sigma phase or secondary phases were not detected as, shown in figure 4. This represents diffraction patterns

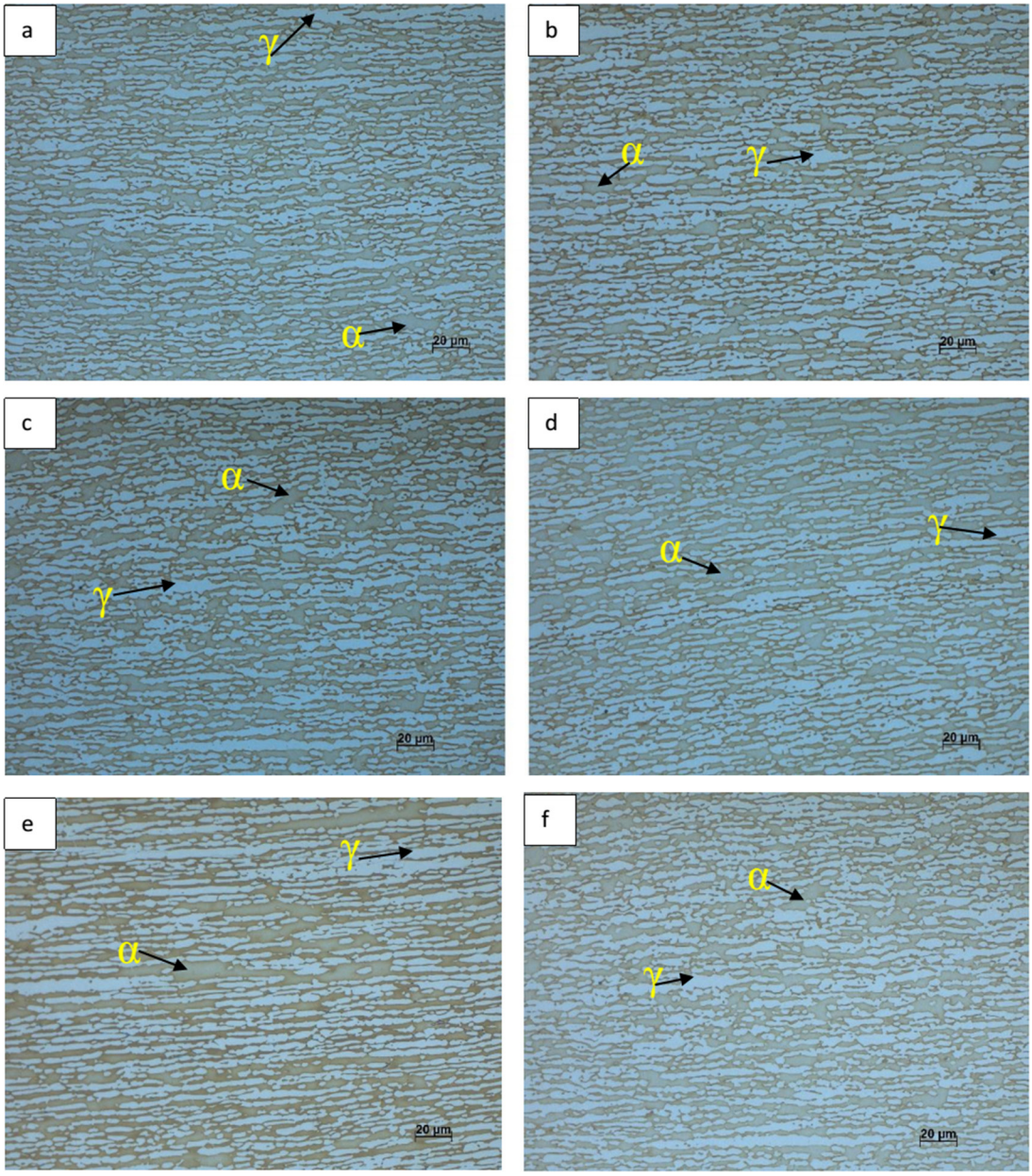

Figure 1. Optical micrographs of SAF 2205 specimens annealed at different conditions, the dark part represents ferrite while the light representing austenite. (a) Untreated (b) 800 °C, 2 min (c) 800 °C, 4 min (d) 800 °C, 8 min (e) 850 °C, 2 min (f) 900 °C, 2 min.

of samples treated at 800 °C for 8 min, 850 °C for 2 min and 900 °C for 2 min, which have agreement with optical microscope and scanning electron microscope images. It proved that the two samples contain the ferrite and austenite phase; no evidence was observed for the sigma phase in the diffraction patterns of the two samples.

The chemical composition of the phases, ferrite, austenite and secondary phases, were determined by energy-dispersive x-ray spectroscopy (EDS) on samples with different aging temperatures and times. Table 3 gives the results of the EDS analysis of each phase of the microstructure of the 2205 DSS. The chemical composition of each phase does not vary much with the composition of the base alloys. The EDS analysis results are presented in table 3, where it is shown that the ferrite phase is rich in chromium and molybdenum with regard to nickel, while the austenite phase enriches in nickel and content chromium and molybdenum lower than the ferrite phase. These results are in good agreement with other authors [18, 19].

3.4. Effect of aging treatment on the micro-hardness

The micro hardness of the aged samples is also studied, as a function of the aging temperature and time. Table 4 describes the influence of ageing treatment on the hardness of the studied 2205 DSS. Vickers micro hardness values of all aged samples ranged from 234 to 264 HV and depended on aging temperature and time. The aging treatment in the temperature range between 750–950 °C for 2, 4, 8 min would not have had a great influence on

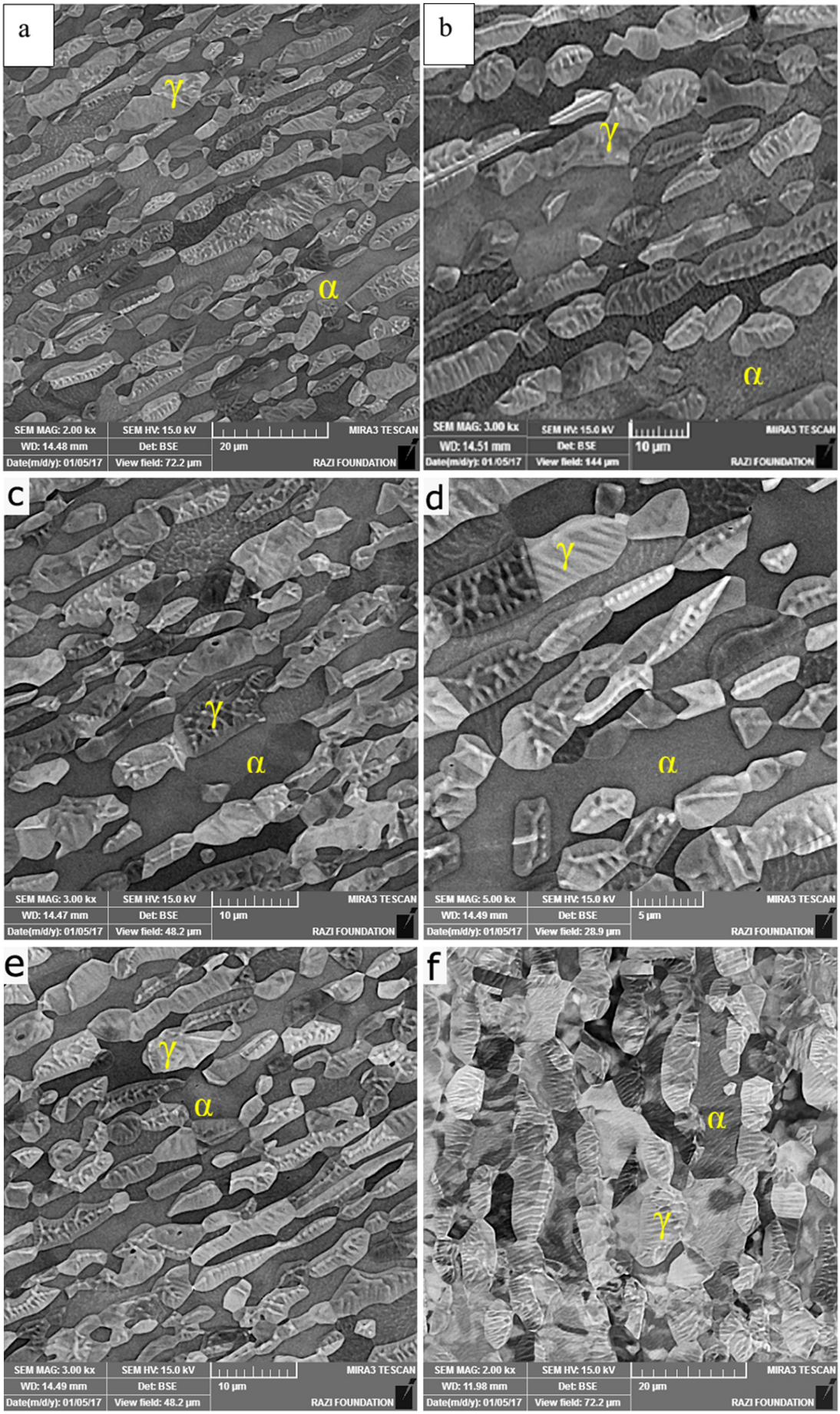

Figure 2. Morphologies of SAF 2205 specimens characterized by SEM, the dark part represents ferrite while the light representing austenite. (a) Untreated (b) 800 °C, 2 min (c) 800 °C, 4 min (d) 800 °C, 8 min (e) 850 °C, 2 min (f) 900 °C, 2 min.

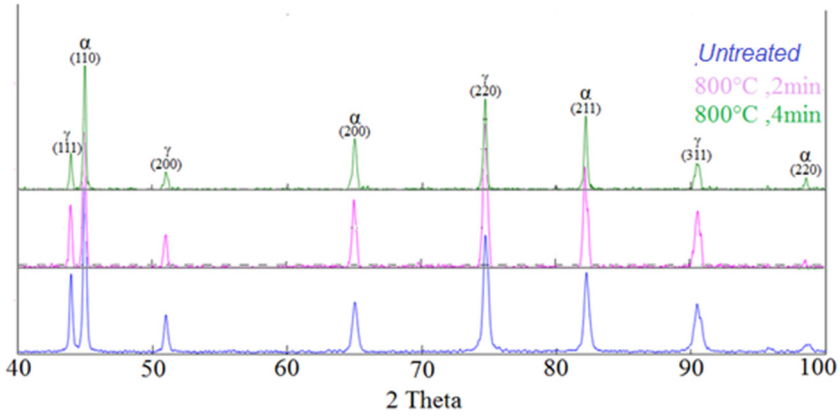

Figure 3. X-ray diffraction pattern of three specimens of 2205 DSS.

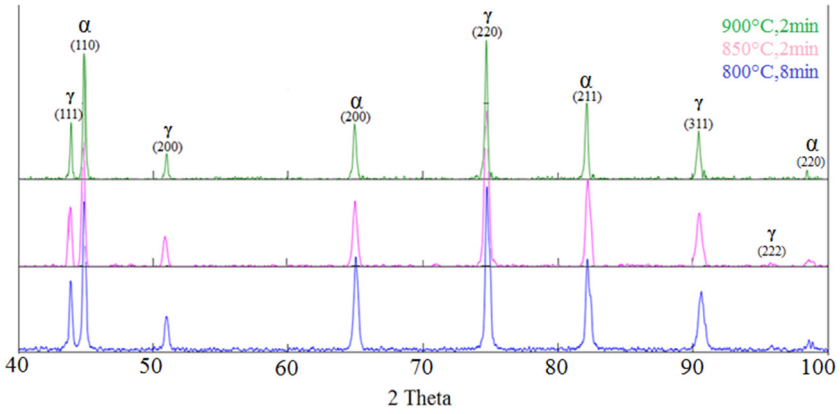

Figure 4. X-ray diffraction pattern of three specimens of 2205 DSS.

Table 3. Chemical composition of various phases obtained by EDS (wt. %).

Treatment condition (°C, min)	Phase	Cr (mean)	Ni (mean)	Mn (mean)	Mo (mean)	Fe (mean)
Untreated	Ferrite	21.53	3.00	0.83	5.31	Balance
	Austenite	16.98	5.53	0.59	3.12	Balance
800, 2	Ferrite	21.23	3.03	0.81	5.86	Balance
	Austenite	17.40	5.65	0.61	3.00	Balance
800, 4	Ferrite	21.61	3.13	0.75	5.65	Balance
	Austenite	18.30	5.30	0.64	3.48	Balance
800, 8	Ferrite	21.46	3.48	0.76	5.54	Balance
	Austenite	18.04	5.53	0.60	3.48	Balance
850, 2	Ferrite	21.07	3.25	0.69	5.55	Balance
	Austenite	18.13	5.52	0.65	3.38	Balance
900, 2	Ferrite	20.77	3.30	0.61	5.23	Balance
	Austenite	18.34	5.52	0.49	3.80	Balance

the volume fraction of ferrite and austenite. Nevertheless, the hardness values of the aged samples were changed with aging temperature and time, which was in agreement with other authors' reports [20].

As an important parameter of mechanical properties, hardness of the aged specimens is also investigated as a function of the aging temperature, plotted in figure 5. Vickers hardness (VH) values of all aged specimens were located in the range of 234–256HV and changed with aging temperature and time. The initial hardness of the untreated sample was 251.5 HV for 2205 DSS. Further ageing at higher temperatures causes precipitation of the sigma phase and significant hardness increase. However, the amount of secondary precipitates formed during the aging process for 2205 DSS alloy was low and appeared only at 900 °C, 850 °C for 8 min. Consequently, the hardness of the aged specimen did not change with the aging temperature.

Table 4. Micro-hardness values with different ageing temperature for different aging time.

Heat treatment conditions							
(°C)	(min)	HV1	HV2	HV3	HV4	HV5	HV average
	Untreated	264	252	258	260	260	259
800	2	250	248	252	253	252	251
800	4	254	254	257	264	251	256
800	8	247	246	241	240	243	243
850	2	246	253	254	249	252	251
900	2	249	238	245	236	234	241

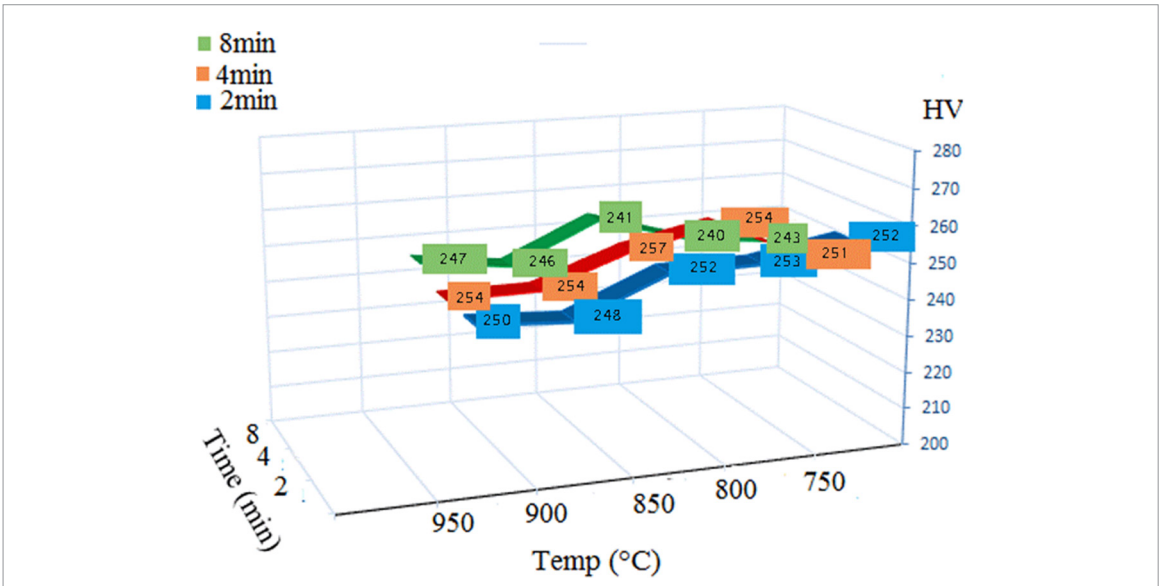

Figure 5. Variation of micro-hardness values with different ageing temperature for different ageing time.

The hardness of the bulk was obtained from its phases' hardness (ferrite, austenite and secondary phases). The hardness of the austenite phase depends on the FCC crystalline cells' distortion, which results from a substitutionally solid solution, which is formed by elements that have a large atomic radius, such as molybdenum, chromium, and nickel [21]. The hardness values mainly depend on the presence or absence of the sigma phase because it is brittle and hard, where its hardness value was as reported by authors. The bulk hardness depends on the phase's fraction in which indentation occurs. The heat treatment at this condition does not cause great changes in the volume fractions of phases in the treated samples; therefore, no significant difference in hardness values is shown in figure 5.

3.5. Effect of heat treatment on corrosion behavior of 2205 DSS

The microstructure change, which occurred due to heat treatment and secondary phases precipitated, plays an important role in the corrosion behavior of DSS alloys, where the heat treatment effect on the corrosion behavior of DSS is due to many factors. The first was precipitation of secondary phases where the formation of the σ phase DSS led to a drastic reduction in its corrosion resistance. The second factor was that it changed the ferrite/austenite ratio where the corrosion occurred preferentially in the ferrite phase of DSSs. The austenite phase has better corrosion resistance than the ferrite phase for many reasons, such as more nickel content than ferrite and, generally, Cr is the most effective element in the passive film to improve the resistance of DSS to localized corrosion where the ferrite phase has more Cr. However, the major alloying element in the austenite phase is Ni, whereas in the ferrite phase it is Cr. Since Cr is more active than Ni, it will probably act as an anode. The corrosion potential of Cr in DSS was lower than the corrosion potential of Ni in active status, therefore chromium was not the main parameter for the difference in the corrosion resistance between the two phases. Additionally, the ferrite phase was electrochemically more active, and these results arise from differences in the chemical compositions of each alloy [22]. Ferrite is relatively rich in Cr and Mo while austenite is rich in Ni and N. Furthermore, nickel has many functions added to control the phase balance and element partitioning, but also to increase the corrosion resistance [8]. From the data shown in table 3, the nickel content in the austenite was more than 5% and it was more than that in the ferrite.

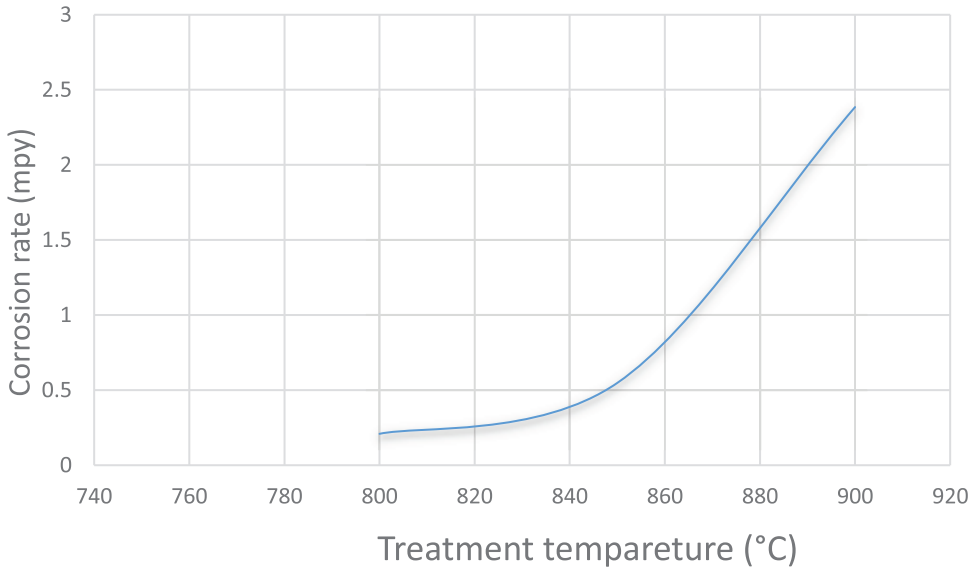

Figure 6. Relationship between aging temperature and corrosion rate at 2 min.

The second reason for the better corrosion resistance for the austenite phase than the ferrite was the higher N solubility due to the higher Mn content. When the ferrite content increases more than the optimum ratio, this will result in reducing in corrosion resistance and when the ferrite decreases less than optimum content. Then this will lead to increasing the chromium and molybdenum in the ferrite phase, which leads to secondary phases' precipitation. The sample has a better microstructure (ferrite/austenite ratio) and has higher corrosion resistance. Figure 6 shows the relationship between the aging temperature and corrosion rate at 2 min, which indicates that the corrosion rate increases when the microstructure is away from the optimum microstructure. The heat-treated samples and as-received potentiodynamic curves in artificial saliva at 37 °C are reported in figure 7.

The results show that the best ferrite/austenite ratio for the studied specimens was obtained after having treated the sample at 900 °C for 2 min. Therefore, this sample has the least current density as shown in table 5 and a higher corrosion resistance. The sample treated at 850 °C for 2 min has a microstructure close to the sample at 900 °C for 2 min; therefore it has corrosion resistance less than the sample at 900 °C for 2 min, but more than other specimens. When the ageing time increased from 2 to 8 min (at 800 °C), the current density reduced from 3.87 to 1.76 μA cm^{-2}. This resulted in the corrosion rate of the specimen treated for 8 min being less than specimen treated for 2 min, due to increasing in the austenite phase fraction. This result is in agreement with other authors [22, 23]. The sample treated at 800 °C, for 4 min has the current density less than sample treated for 2 min and more than sample treated for 8 min.

Table 5 describes the electrochemical parameters' values obtained from potentiodynamic polarization, which indicated that the sample treated at 900 °C for 2 min has the best corrosion resistance properties and the sample treated at 800 °C for 2 min has the lowest corrosion resistance properties.

3.6. Cyclic polarization of 2205 DSS in artificial saliva

The electrochemical behavior of 2205 DSS in artificial saliva, before and after ageing treatment, was analyzed by cyclic potentiodynamic polarization. In this, the polarization curve consists of a forward scan as well as a backward scan starting at an active OCP. The OCP (E_{corr}) for 2205 DSS in artificial saliva after ageing, was approximately 200 mV. The pitting potential (E_p) is defined as the potential at which the anodic current density increased sharply with respect to the backward scan and the passive current density. The protection potential (E_{prot}) is the noblest potential where pitting and crevice corrosion will not propagate and at which re-passivation occurs, or it is the potential at which the reverse scan intersects the forward scan at a value that is less noble than E_p. If E_{prot} is high or more anodic, that is minimal hysteresis, then the metal is said to be very resistant to crevice corrosion [13, 24]. ΔE ($E_p - E_{prot}$) represents the corrosion resistance of the materials and the smaller the ΔE value, the better the anti-corrosion property.

Cyclic potentiodynamic polarization analyzed the electrochemical behavior of 2205 DSS in artificial saliva at 37 °C before and after ageing treatment. Figure 8 illustrates the cyclic potentiodynamic polarization curves of 2205 DSS specimens in artificial saliva solution. It shows that the sample treated at 900 °C for 2 min has the best pitting corrosion resistance. It has the highest breakdown or pitting potential, as shown in table 6, which illustrates the electrochemical parameters of 2205 DSS before and after heat treatment obtained in artificial saliva solution with cyclic polarization. Furthermore, it has the highest protection or re-passivation potential (−58.3

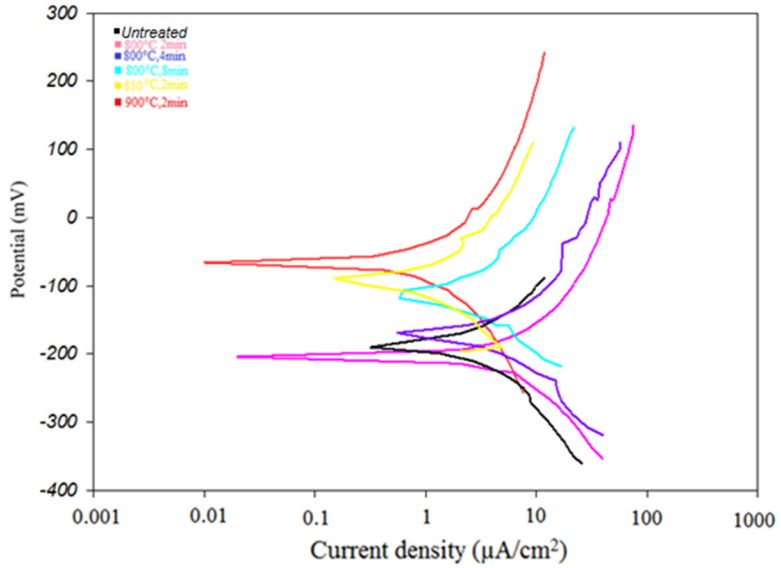

Figure 7. Potentiodynamic polarization curves of 2205 DSS samples in artificial saliva at 37 °C.

Table 5. Corrosion data obtained from the electrochemical tests at room temperature in artificial saliva.

Treatment conditions		Current density (μA cm^{-2})	Corrosion rate (mpy)
	Untreated	2.12	0.890
800 °C	2 min	3.87	1.625
800 °C	4 min	2.92	1.226
800 °C	8 min	1.76	0.663
850 °C	2 min	1.02	0.428
900 °C	2 min	0.77	0.325

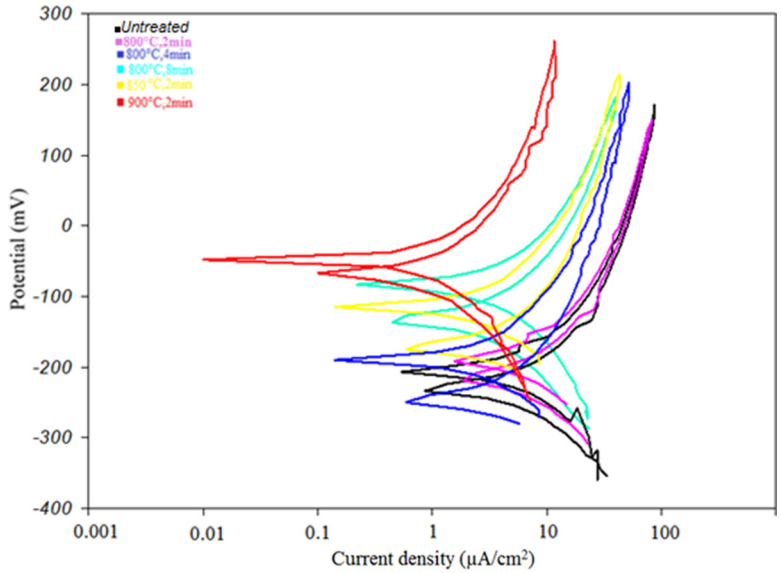

Figure 8. Cyclic potentiodynamic polarization curves of 2205 DSS specimens in artificial saliva solution.

mV). This means that the repair of protective film and re-passivation process occurs more readily when it is compared with other specimens. The sample has a microstructure nearest to the microstructure sample treated at 900 °C for 2 min. When treated at 850 °C for 2 min, it has pitting potential (205 mV), this gives evidence that the pitting resistance depends on microstructure. The specimen which has the lowest pitting corrosion resistance was treated at 800 °C for 2 min and has pitting potential of about (150 mV). With a sample that has a lower value of ΔE ($E_p - E_{prot}$), if the pitting occurred the propagation happened in a smaller voltage range, as in the specimen treated at 800 °C for 8 min.

Table 6. Electrochemical parameters of 2205 DSS before and after heat treatment obtained artificial saliva solution with cyclic polarization.

Aging temperature	Aging time	E_{corr} (mV)	E_p (mV)	E_{prot} (mV)	ΔE ($E_p - E_{prot}$) (mV)
Untreated		−207.0	173.0	−216.6	389.0
800 °C	2 min	−195.0	150.0	−201.0	351.0
800 °C	4 min	−189.0	202.0	−218.7	420.0
800 °C	8 min	−95.0	182.0	−105.0	287.0
850 °C	2 min	−115.0	205.0	−145.0	350.0
900 °C	2 min	−48.6.0	263.8	−59.8	323.0

Table 7. Nickel ion released from the 2205 DSS specimen.

Treatment conditions		Ni ion released (ppm)	Accumulated Ni released rate (μg cm^{-2})	Accumulated Ni released (μg)
Untreated		0.070	1.050	2.110
800 °C	2 min	0.076	1.140	2.280
800 °C	4 min	0.052	0.780	1.570
800 °C	8 min	0.067	1.010	2.030
850 °C	2 min	0.042	0.630	1.260
900 °C	2 min	0.028	0.420	0.850

3.7. Effect of aging treatment on the nickel ion released for 2205 DSS in artificial saliva

Amounts of nickel ions released from the 2205 DSSs in artificial saliva at 37 °C versus immersion time was 28 d, as shown in table 7. All tested specimens have accumulated Ni released with safe limits that were less than the normal daily intake 200–300 μg d^{-1} [25, 26].

The amounts of nickel released from all samples were much less than the safe limit and less than the amount released from 316 SS. The amount of Ni released by the specimen in table 7 was less than the amount of Ni released for 316 SS [13]. This has an advantage in biocompatibility, thus could have decreased nickel sensitivity caused by orthodontic wire. As mentioned previously, the heat treatment affected the microstructure (changed the austenite/ferrite ratio and may have precipitated a secondary phase), and this had an influence on the corrosion resistance of DSS alloys specimens. The sample was treated at 900 °C for 2 min, which has a balance microstructure. The last four specimens in table 7 released nickel ions lower than the specimen before heat treatment.

4. Conclusions

1- The current outcomes have shown that SAF 2205 have excellent resistance to corrosion. This makes them valuable for a particular application, especially in the orthodontic field.
2- Aging temperature and aging time and chemical composition have important roles in secondary phase precipitations and phases' balance in the 2205 DSS.
3- The ferrite phase was more inclined to corrosion than the austenite phase, indicating that ferrite acts as a preferential anode to the austenite phase. Polarization measurements confirm this observation, and proved that ferrite may behave as a net anode.
4- The 2205 DSS has higher corrosion resistance when treated at 900 °C, 2 min, but when treated at 800 °C, 2 min has least corrosion resistance. The optimum manipulation in both of heat treatment (aging temperature and aging time) and chemical composition lead to optimum balance in the microstructure of DSS.
5- Nickel hypersensitivity and content represent an annoying issue in the medical treatment field, and the mitigation of such problems will be helpful in the mentioned filed. After conducting the current study, both of them are reduced significantly in 2205 DSS. These outcomes could be interpreted as a stability or suitability of these materials for medical purposes.

AQ4 ## Acknowledgment

The authors would like to thank to assisting in the practical part by Dr Raid Abdul Abbas, Research Engineer-High Performance Stainless and Alloys-Avesta Research Center—Outokumpu Stainless AB, Avesta, Sweden and Al-Razi metallurgy research center-Iran.

ORCID iDs

Ali Sabea Hammood https://orcid.org/0000-0002-0047-2900

AQ5

References

[1] Deng B, Jiang Y, Gong J, Zhong C, Gao J and Li J 2008 Critical pitting and re-passivation temperatures for duplex stainless steel in chloride solutions *Electrochim. Acta* **53** 5220–5

[2] Igual Munoz A, Garcia Anton J, Guinon J L and Perez Herranz V 2007 Inhibition effect of chromate on the passivation and pitting corrosion of a duplex stainless steel in LiBr solutions using electrochemical techniques *Corros. Sci.* **49** 3200–25

[3] Igual Munoz A, Garcia Anton J, Guinon J L and Perez Herranz V 2006 The effect of chromate in the corrosion behavior of duplex stainless steel in LiBr solutions *Corros. Sci.* **48** 4127–51

[4] do Nascimento A M, Ierardi M C F, Kina A Y and Tavares S S M 2008 Pitting corrosion resistance of cast duplex stainless steels in 3.5%NaCl solution *Mater. Charact.* **59** 1736–40

[5] Moura V S, Lima L D, Pardal J M, Kina A Y, Corte R R A and Tavares S S M 2008 Influence of microstructure on the corrosion resistance of the duplex stainless steel UNS S31803 *Mater. Charact.* **59** 1127–32

[6] Sathirachinda N, Pettersson R and Pan J 2009 Depletion effects at phase boundaries in 2205 duplex stainless steel characterised with SKPFM and TEM/EDS *Corros. Sci.* **51** 1850–60

[7] Ebrahimi N, Momeni M, Moayed M H and Davoodi A 2011 Correlation between critical pitting temperature and degree of sensitisationon alloy 2205 duplex stainless steel *Corros. Sci.* **53** 637–44

[8] Liou H Y, Pan Y T, Hsieh R I and Tsai W T 2001 Effects of alloying elements on the mechanical properties and corrosion behaviors of 2205 duplex stainless steels *J. Mater. Eng. Perform.* **10** 231–41

[9] Yang S M, Chen Y C, Pan Y T and Lin D Y 2016 Effect of silver on microstructure and antibacterial property of 2205 duplex stainless steel *Mater. Sci. Eng.* C **63** 376–83

[10] Jinlong L, Tongxiang L, Chen W and Limin D 2016 Effect of ultrafine grain on tensile behavior and corrosion resistance of the duplex stainless steel *Mater. Sci. Eng.* C **62** 558–63

[11] Vignal V, Zhang H, Delrue O, Heintz O, Popa I and Peultier J 2011 Influence of long-term ageing in solution containing chloride ions on the passivity and the corrosion resistance of duplex stainless steels *Corros. Sci.* **53** 894–903

[12] Wang Y, Cheng X and Li X 2015 Electrochemical behavior and compositions of passive films formed on the constituent phases of duplex stainless steel without coupling *Electrochem. Commun.* **57** 56–60

[13] Sobol O, Holzlechner G, Nolze G, Wirth T, Eliezer D, Boellinghaus T and Unger W E 2016 Time-of-flight secondary ion mass spectrometry (ToF-SIMS) imaging of deuterium assisted cracking in a 2205 duplex stainless steel microstructure *Mater. Sci. Eng.* A **676** 271–7

[14] Kocijan A, Merl D K and Jenkoet M 2011 The corrosion behavior of austenitic and duplex stainless steels in artificial saliva with the addition of fluoride *Corros. Sci.* **53** 776–83

[15] Calliari I, Pellizzari M, Zanellato M and Ramous E 2011 The phase stability in Cr–Ni and Cr–Mn duplex stainless steels *J. Mater. Sci.* **46** 6919–20

[16] Badji 1-R, Bouabdallah M, Bacroix B, Kahloun C, Bettahar K and Kherrouba N 2008 Effect of solution treatment temperature on the precipitation kinetic of-phase in 2205 duplex stainless steel welds *Mater. Sci. Eng.* A **496** 447–54

[17] Fargas G, Anglada M and Mateo A 2009 Effect of the annealing temperature on the mechanical properties, formability and corrosion resistance of hot-rolled duplex stainless steel *J. Mater. Process. Technol.* **209** 1770–82

[18] Chen T H, Weng K L and Yang J R 2002 The effect of high-temperature exposure on the microstructural stability and toughness property in a 2205 duplex stainless steel *Mater. Sci. Eng.* A **338** 259–70

[19] Calliari I, Zanesco M and Ramous E 2006 Influence of isothermal aging on secondary phases precipitation and toughness of a duplex stainless steel SAF 2205 *J. Mater. Sci.* **41** 7643–9

[20] Deng B, Wang Z, Jiang Y, Sun T, Xu J and Li J 2009 Effect of thermal cycles on the corrosion and mechanical properties of UNS S31803 duplex stainless steel *Corros. Sci.* **51** 2969–75

[21] Martins M and Casteletti L 2005 Heat treatment temperature influence on ASTM A890 GR 6A super duplex stainless steel microstructure *Mater. Charact.* **55** 225–33

[22] Park C J, Kwon H S and Lohrengel M M 2004 Micro-electrochemical polarization study on 25% Cr duplex stainless steel *Mater. Sci. Eng.* A **372** 180–5

[23] Ahn Y S and Kang J P 2000 Effect of aging treatments on microstructure and impact properties of tungsten substituted 2205 duplex stainless steel *Mater. Sci. Technol.* **16** 382–8

[24] Luo H, Dong C F, Xiao K and Li X G 2011 Characterization of passive film of 2205 duplex stainless steel in sodium thiosulphate solution *Appl. Surf. Sci.* **258** 631–9

[25] Kuhta M, Pavlin D, Slaj M, Varga S, Lapter M and Slaj M 2008 Type of arch wire and level of acidity: Effects on the release of metal ions from orthodontic appliances *Angle Orthod.* **79** 102–10

[26] Eliades T and Athanasiou A 2002 *In vivo* aging of orthodontic alloys: implications for corrosion potential, nickel release, and biocompatibility *Angle Orthod.* **72** 222–37

[27] Lee T H, Huang T K, Lin S Y, Chen L K, Chou M Y and Huang H H 2010 Corrosion resistance of different nickel-titanium arch wires in acidic fluoride-containing artificial saliva *Angle Orthod.* **80** 547–53

[28] Mitchell L 2013 *An introduction to Orthodontics* 4th edn (Oxford: Oxford University Press)